# A Risk-Resilience Calculation Method for Environmental Change and Disaster Analysis with 5D World Map System Visualization

Shiori Sasaki,[1,2] Yasushi Kiyoki,[1,2] Amane Hamano[2]

[1] Keio University, Tokyo, Japan
{ssasaki, y-kiyoki}@musashino-u.ac.jp
[2] Musashino University, Tokyo, Japan
{ssasaki, y-kiyoki}@musashino-u.ac.jp, s2122067@stu.musashino-u.ac.jp

This paper presents an important application of 5D World Map System, which realizes an analytical computing and visualization for expressing environmental phenomena, causalities and influences, with "Time-series Multilayer Risk-Resilience Calculation" method for global environmental change and disaster analysis to make appropriate and urgent solutions to global and local environmental phenomena in terms of short and long-term changes. This method enables the calculation of the current risk and resilience of a target region or city to disasters based on the history of past time-series changes and the overlap of multidimensional factors to predict them in the near future. This method calculates the total risk and resilience to disaster as a total aggregate value that reflects the amount of change in each variable in the past, by transforming multidimensional and heterogeneous variables into a form that allows comparative and arithmetic operations through normalization. As an implementation and experiments, we apply our method to assessing the role of forests in urban disaster resilience by analysing the relationships between time-series changes in forest distribution and urban disaster occurrence, specifically using GIS, satellite data, demographic data, urban infrastructure data, and disaster data and calculate "urban-forest-disaster risk/resilience".

**Keywords:**
CPS, cyber-physical-system, sensing-processing-actuation, GIS, open data, visualization, knowledge bases, SDGs, SDG9, SDG11, SDG13, SDG15, deforestation, disaster risk, disaster resilience, urban development, global environment

University of Maribor Press

DOI https://doi.org/10.18690/um.feri.5.2023.16
ISBN 978-961-286-745-4

## 1 Introduction

Disaster Risk Reduction (UNDRR) points out [19], it is essentially important to collect disaster information in a wide area in real time, to make it accessible and public through open data, and to detect vulnerable areas at an early stage and take countermeasures for the realization of Sustainable City (SDG9, SDG11) and Disaster Resilience (Sendai Framework [20]). In fact, many cases have been reported where it is difficult to accurately assess the current situation and identify disaster-risk hotspots due to lack of information and data.

In addition, not only detecting disaster-risk hotspots but also estimating disaster-resilience is an important and urgent task to build capacity. As Sendai Framework [20] indicates, it is important to make "action to prevent new and reduce existing disaster risks: (i) Understanding disaster risk; (ii) Strengthening disaster risk governance to manage disaster risk; (iii) Investing in disaster reduction for resilience and (iv) Enhancing disaster preparedness for effective response, and to "Build Back Better" in recovery, rehabilitation and reconstruction."

One possible solution to these issues is the use of satellite multispectral imagery and open data of socioeconomics to detect the risk and vulnerability of the specific area of the countries with rapid environmental changes and disasters.

The objective of our method is not only to visualize but also to calculate the risk/vulnerability and the resilience of society for disaster risks in a target area as values to make appropriate and urgent solutions to global and local environmental phenomena in terms of short and long-term changes, with a time-series and multi-layered manners.

In this study, we describe a method of "Time-series Multi-layered Risk-Resilience Calculation" for estimating the risk or resilience of a (possible) disaster-affected area using open satellite data and remote sensing technology. This method enables the calculation of the current risk and resilience of a target region or city to disasters based on the history of past time-series changes and the overlap of multidimensional factors, and to predict them in the near future.

In the implementation, we focus on deforestation and landslide phenomena, which are considered to be caused by a combination of natural disasters such as heavy rainfall, floods, earthquakes, and human socio-economic activities such as land-use development, logging, farming, building etc. We describe the feasibility and effectiveness of our method by several experiments with the data of (a) landslide and flood risks, (b) population growth, (c) infrastructure development and (d) forest distribution in Japan (Ibaraki Prefecture in Japan, 2015 and 2020).

The Time-series Multi-layered Risk-Resilience Calculation method realized by this study is designed to be applied to the 5D World Map System [1]-[8].

"SPA-based 5D World Map System" [1]-[8] is a global and environmental knowledge-integrating and processing system for memorizing, searching, analysing and visualizing "Global and Environmental Knowledge and Information Resources," related to natural phenomena and disasters in global and local environments. This system analyses environmental situations and phenomena with "environmental multimedia data sharing," as a new global system architecture of collaborative and global environment analysis. This system realizes a remote, interactive and real-time environmental research exchange among different areas.
On the other hand, in the field of the remote sensing, many studies have been conducted to estimate environmental changes on the earth surface and the land use status using environmental indices such as the Normalized Difference Vegetation Index (NDVI) Normalized Difference Water Index (NDWI), Normalized Difference Snow Index (NDSI) by using satellite multispectral imagery. We utilize these remote sensing techniques and apply them to create knowledge bases for our objectives in this study.

In addition, our method utilizes open-data satellite multispectral imagery to estimate the size of disaster-affected area with relatively high accuracy using an inexpensive and uncomplicated estimation method. This feature makes the method widely applicable to LDCs and small local governments. In particular, the method is effective for early assessment of the situation, such as rapid confirmation of the disaster situation in wide-area disasters.

In this paper, we focus on the deforestation and landslide disasters as an example and conduct an implementation and experiments using open satellite data and open-source GIS software. Furthermore, the applicability of our method to a multi-dimensional world map system is also discussed.

## 2 Overview of SPA-based 5D World Map System

5D World Map System [1]-[8] is a knowledge representation system that enables semantic, temporal and spatial analysis of multimedia data and integrates the analysed results as 5-dimentional dynamic historical atlas (5D World Map). The composition elements of 5D World Map are a spatial dimension (3D), a temporal dimension (4D) and a semantic dimension (5D).

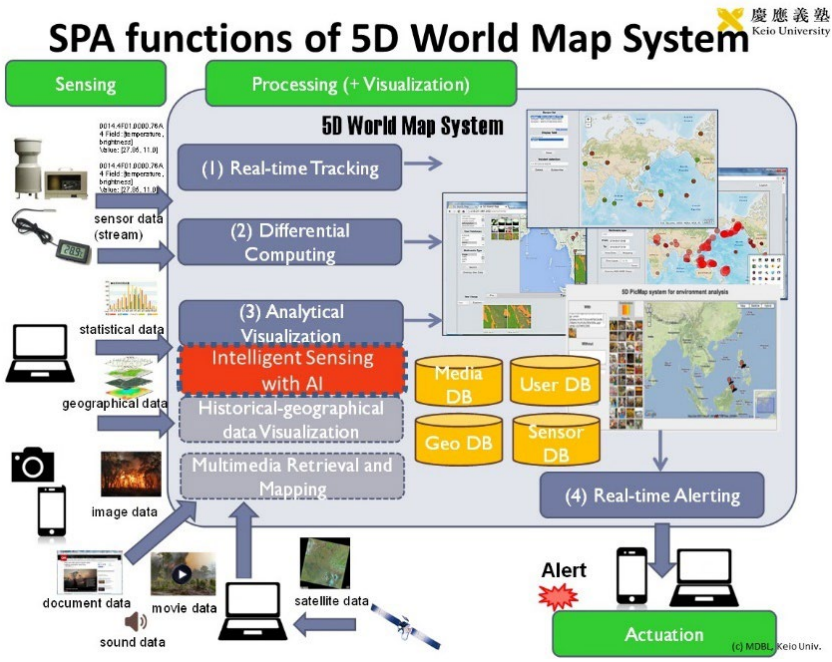


**Figure 1: System Structure of 5D World Map System with AI-Sensing**
Source: [33].

A semantic associative search method [9][10] is applied to this system for realizing the concept that "semantics" of words, documents, multimedia, events and phenomena vary according to the "context". 5D World Map System [1]-[8] has been providing various functionalities to calculate and express the semantics and context

of various types of multimedia data [4][5][7][8]. Also, the functions for monitoring, analysing and warning with a multi-dimensional and multi-layered visualization of 5D World Map System with AI-Sensing has been utilized for monitoring SDG14, SDG9, SDG11 (Sustainable Ocean and Disaster Resilience) in United Nations ESCAP [7][31][32][33]. The SPA (Sensing-Processing-Actuation) process of 5D World Map System is shown in **Figure 1**.

Currently, the 5D World Map System is globally utilized as a Global Environmental Semantic Computing System, in SDG14, United-Nations-ESCAP's Closing-The-Loop project [32] for observing ocean-environment situations with local and global multimedia data resources [33]. In this project of plastic garbage detection and reduction, we include a new function of AI-Sensing to 5D World Map System and apply the analytical visualization functions in the SPA (Sensing-Processing-Actuation) process as shown in **Figure 1**.

## 3 Related Studies

### 3.1 Multilayer Visualization with 5D World Map System

The multilayer visualization function of 5D World Map System and its application for ocean environmental analysis [7] and disaster-resilience monitoring [8] have been presented. Our method described in this paper is based on these research results on methods for analyzing and predicting disaster resilience from the interaction of global and local views [7][8].

### 3.2 Multispectral Image Analysis with 5D World Map System

SPA-based environmental-semantic computing for global and local environment analysis with multispectral image analysis [2] and its application for coral health monitoring [11][13] have been proposed. Also, the deforestation analyses with satellite multispectral images and SAR data analysis [12][14][17] applied to 5D World Map System, and multispectral imaging with UAV for agricultural monitoring and analysis [16][18] have been proposed.

### 3.3 Disaster Risk Analysis

There are many disaster risk visualization systems and disaster prevention maps using multispectral satellite imagery and remote sensing, and there are also open data platforms on disasters provided by national and local governments [21][22][23][24]. On the other hand, individual studies on estimating and visualizing the actual disaster area using these technologies are scattered locally in the fields of GIS, disaster prevention, and environmental engineering. However, a globally aggregated information platform with disaster data analysis, visualization, and sharing systems are still in the research and development stage [25].

Also, there are a lot of studies on disaster risk detection using satellite multispectral imagery and remote sensing. For example, a study using high-resolution satellite images to predict the risk of landslides by evaluating the predisposition to landslides from satellite images has proposed [26]. Another study proposed the extraction of reflectance characteristics that are highly relevant to landslide risk using visible and infrared images from multispectral imagery as well as our method [27]. In their research paper, they presented disaster damage prediction at the time of the shooting using highly accurate satellite multispectral imagery.

About the cause and effect of deforestation, there is a study which discusses the causes of deforestation in the tropical areas from the aspects of slash-and-burn agriculture, population growth, poverty, and road construction [29]. Based on this reference, we focus on population growth and road construction in the implementation, which are also cited as causes of deforestation even in the non-tropical area. We visualize their relationship with forests in the Kanto region (Ibaraki prefecture) in Japan to show the importance of forests and their effects and impacts. There is another study which analyzes of the relationship between the development of urbanization on steep slopes and landslides [30]. In this study, we focus on the increasing risk of landslides including rainfall factors because urban residential development is approaching steep slopes and the damage often occurs in residential areas adjacent to these slopes.

From a technical aspect, satellite image analysis methods using opensource GIS software, QGIS, are widely introduced [28][42]. In this study, we refer to the method of using and utilizing QGIS and show the possibility of integrated use with various open data.

In this study, we design and implement a method to analyze and visualize the relationship between disasters and forests in urban areas in a multilayered manner, focusing on the geographical system characteristics, land use change, and landslide characteristics in urban areas.

## 4 Time-series Multilayered Risk-Resilience Calculation Method for Environmental Changes and Disasters

Our method of Time-series Multilayered Risk-Resilience Calculation is assumed to be applied to the 5D World Map System [1]-[8]. **Figure 2** shows the overall configuration of a multi-dimensional map visualization system (5D World Map System) for disaster data to which this method is applied.

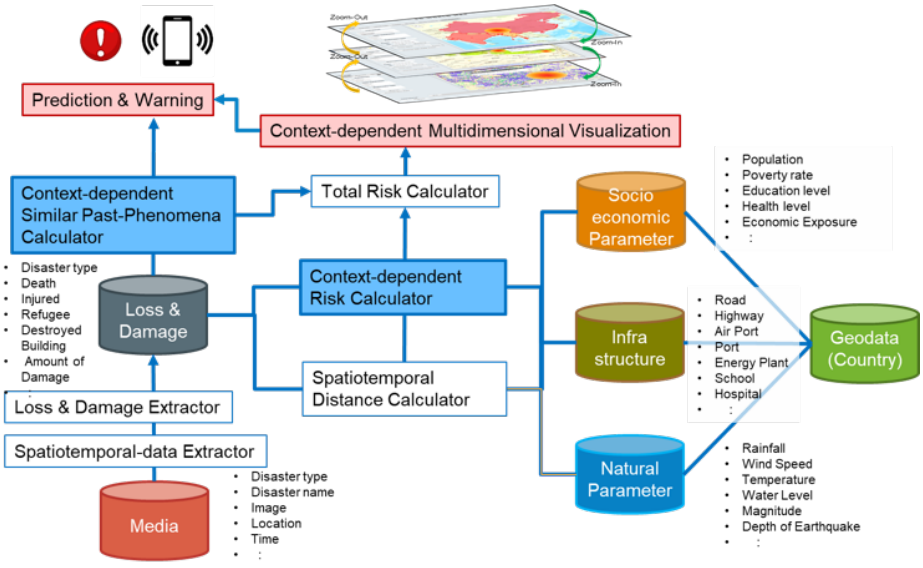


**Figure 2: System structure of Multidimensional World Map System (5D World Map System) [8] to which our Time-series Multilayered Risk-Resilience Calculation method is applied**
Source: [8].

By applying our Time-series Multilayered Risk-Resilience Calculation method to a 5D World Map System, disaster risk calculation and prediction by disaster type can be realized using the Geo Database including Socioeconomic Parameter DB, Infrastructure DB and Natural Parameter DB shown in **Figure 2** and **Figure 3**.

### 4.1 System Architecture

Our Time-series Multilayered Risk-Resilience Calculation method is planned to be implemented as a sub-system (Sub-system 1) of a multidimensional World Map system called "5D World Map System". **Figure 3** shows the total design of sub-systems and the connection to 5D World Map System.

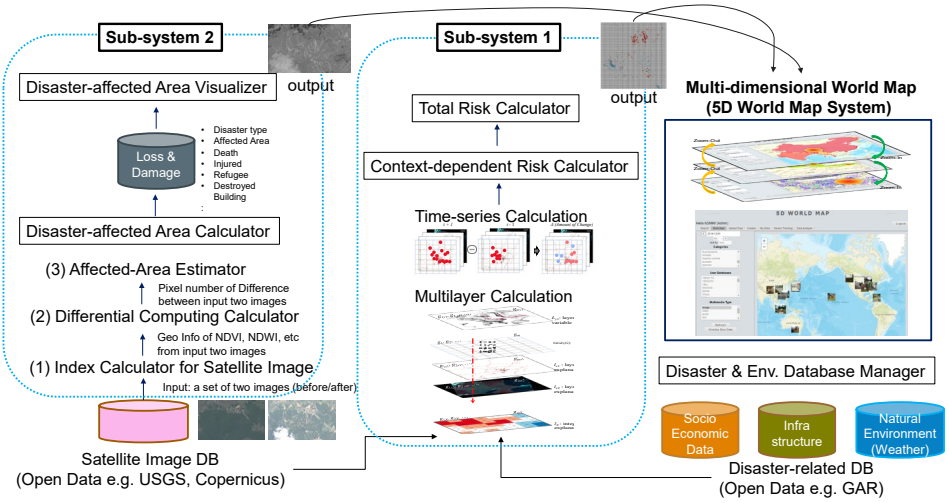


**Figure 3: System structure applying our method as a Sub-system of 5D World Map System**
Source: own.

This system consists of the following functions.

1) *Disaster database management function*: This function is to register and manage metadata such as images and multispectral images collected for the target area, environmental sensing data, statistical data, and infrastructure geographic data.
2) *Time-series Multilayered Risk-Resilience Calculation (Sub-system 1)*
3) *Disaster-affected area estimation & visualization function* [34] *(Sub-system 2)*

4) *Multi-layer visualization function*: Based on the results obtained by functions of 2) and 3), the other data stored in 1) such as environmental sensing data, statistical data, infrastructure geographic data, etc. are projected on the map as multiple layers.

### 4.2 Multilayer Risk-Resilience Calculation

The part of multilayer calculation of the Time-series Multilayered Risk-Resilience Calculation method is defined as the following 6 steps. **Figure 4** shows the visual image of the steps. This process normalizes multidimensional, distributed and heterogeneous variables in a grid format and calculates the total disaster risk/resilience of a specific region as an aggregate value.

STEP 1: Set a phenomenon with spatiotemporal information as an objective variable $y$ and set multiple phenomena with spatiotemporal information as explanatory valuables ($x_1$, $x_2$, …, $x_n$).

STEP 2: Collect geographical information data of $y$ and $x_1$, $x_2$, …, $x_n$. Commonly used geographical information data are Vector data (point/line/polygon, shape file), Raster data (image, GeoTIFF file), Mesh data (AAIGrid file), Point Cloud data, CSV text and KML/KMZ.

STEP 3: Set each geographical information data of each variable as a layer $l_i$ for a geographical information system (GIS). The set of layers are defined as $l_y$ and $l_{x1}$, $l_{x2}$, …, $l_{xn}$.

STEP 4: To enable a calculation of risk or resilience among layers with various granularity, set a common grid $G:=\{g_1, g_2, \ldots, g_m\}$ . The values of each layer's grids (e.g. density of points, pixel value etc.) are expressed as a matrix or a vector such as $l_{y1} = (g_{1y1}, g_{2y1}, \ldots, g_{my1})$, $l_{x1} = (g_{1x1}, g_{2x1}, \ldots, g_{mx1})$, $l_{x2} = (g_{1x2}, g_{2x2}, \ldots, g_{mx2})$ and so on.

STEP 5: Normalization for each layer $l_y$ and $l_{x1}$, $l_{x2}$, …, $l_{xn}$

STEP 6: Create an integrated layer of explanatory variables $l_X$ by calculating a total risk or resilience value $g_{iX}$ with a performance of arithmetic operators (+, -, *, /) for each grid value. For example, the accumulation of values is performed, the created layer $l_X$ and each grid's value $g_{iX}$ of the layer are expressed as:

$$g_{iX} = \sum^{n} (g_{ixi})$$

$$l_X = (g_{1X}, g_{2X}, \ldots, g_{mX}) \quad i=1$$

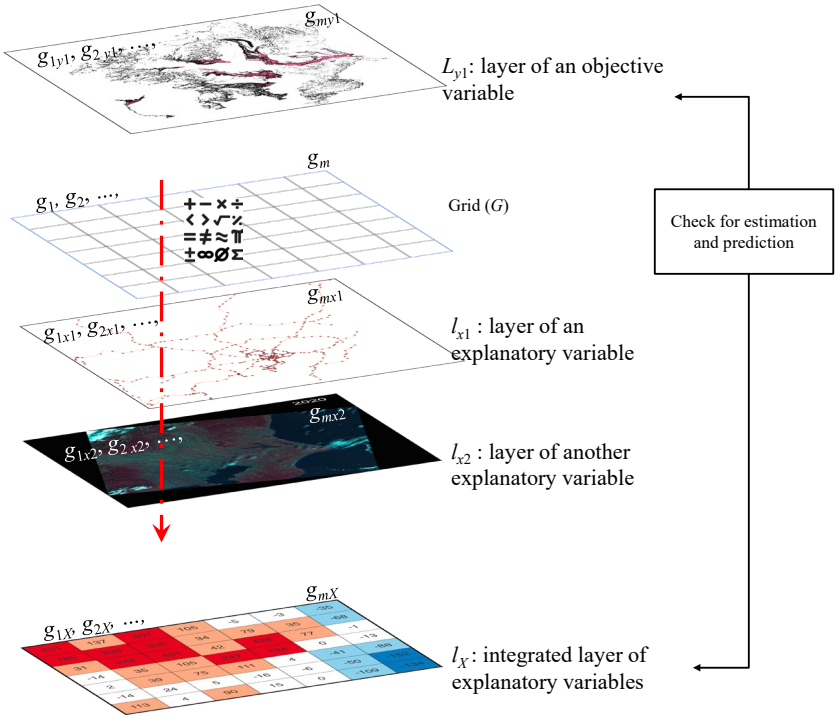


**Figure 4: Multilayer Calculation of Risk-Resilience**

Source: own.

## 4.3 Time-series Risk-Resilience Calculation

The part of time-series calculation of the Time-series Multilayered Risk-Resilience Calculation method is defined as the following 4 steps. **Figure 5** shows the visual image of the steps. The process calculates the time-series change of each variable in a normalized grid format among a multidimensional, distributed and heterogeneous set of variables of disaster risk/resilience in the target area.

STEP 1: Set a phenomenon with spatiotemporal information as an objective variable $y$ and set multiple phenomena with spatiotemporal information as explanatory valuables ($x_1$, $x_2$, …, $x_n$).

STEP 2: Collect geographical information data of $y$ and $x_1$, $x_2$, …, $x_n$, before ($t_i$ - 1) and after ($t_i$ + 1) the time ($t_i$) when disaster or environmental change occurs in the target area.

STEP 3: Set each geographical information data of each variable as a layer $l_i$ for a geographical information system (GIS). The set of layers are defined as $l_y$ and $l_{x1}$, $l_{x2}$, …, $l_{xn}$.

STEP 4: Calculate the difference between the layers of before ($t_i$ - 1) and after ($t_i$ + 1).

STEP 5: If there are many times when disasters or environmental changes occur ($t_i$ | $i$ = 1, 2, …, $q$), the STEP 4 is repeated among ($t_1$-1), ($t_1$+1), ($t_2$+1), …, ($t_q$+1).

For the detection of disaster effect or environmental change using raster data (image, GeoTIFF file), this method uses the "Normalized Difference Environmental Index" such as Normalized Difference Vegetation Index (NDVI), Normalized Difference Water Index (NDWI), Normalized Difference Snow Index (NDSI), Normalized Burn Ratio (NBR), Normalized Difference Built-up Index (NDBI), etc., especially to estimate the size of disaster-affected area before and after the phenomenon happens. Each of these indexes is used to detect environmental changes such as landslides, floods, avalanches, wide-area forest fires and reduction of cultivated land due to buildings.

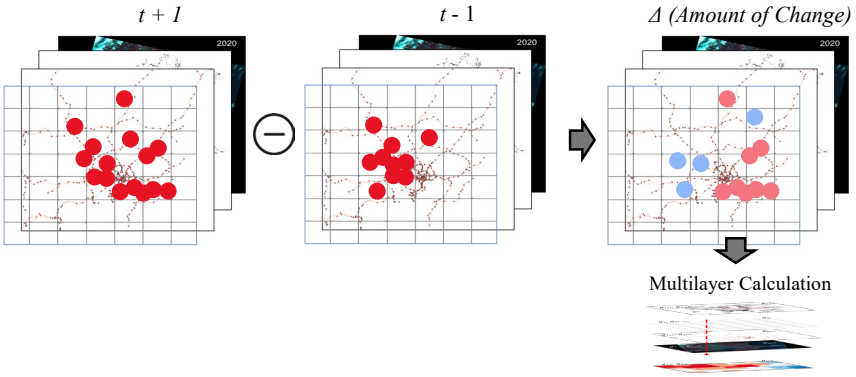


**Figure 5: Time-series Calculation of Risk-Resilience**
Source: own.

## 5 Implementation

To realize our method of Risk-Resilience Calculation, we implement the following process with distributed time-series geographic information data, such as socioeconomic indicator data, demographic data, natural disaster data, urban infrastructure data and satellite image data. In this implementation, we apply our method to assessing the role of forests in urban disaster resilience by analyzing time-series changes in vegetation and forest distribution and their relationships in urban areas. Specifically, using GIS, satellite data, demographic, urban infrastructure, and disaster data, we analyze the relationship among disaster occurrence and 1) population density, 2) urban infrastructure development, and 3) forest distribution. From the results of this analysis, we evaluate the relationship among forest, urban development and natural disasters (hereinafter referred to as "forest-urban-disaster resilience").

In this implementation, the Time-series Multilayered Risk-Resilience Calculation is specifically realized by the following steps using GIS.

STEP 1: Visualize the base near-infrared band (NIR) using satellite multispectral imagery of the target area.
STEP 2: Calculate and visualize vegetation indices (NDVI) using satellite multispectral imagery.
STEP 3: Create virtual layers by incorporating open geographic information data such as demographics, urban infrastructure, and disaster data for the target area.
STEP 4: By switching virtual layers and overlaying them with the base map, the time-series multilayer risk-resilience is calculated to analyze "forest-urban-disaster resilience".
STEP 5: Zoom in on a part of the target area where a major change is observed to confirm the details of the relationship among forests, urban development, and natural disasters.

### 5.1 Data and Tools

In this implementation, the Time-series Multilayered Risk-Resilience Calculation is concretely realized for the following four types of data.

1. Using satellite multispectral images, vegetation distribution is calculated, and time-series changes (differences) are calculated.
2. Population growth rate is measured from time-series population data as demographic data.
3. As urban infrastructure data, geographic data of highway construction is used to overlay the vegetation distribution base map.
4. Data on sediment, flood, and inundation hazard zones will be used as disaster risk data to overlay the vegetation distribution base map.

QGIS [42], an open-source GIS, is used. The concrete data used for experiments are introduced in Section 6.

## 5.2 Data Processing

### 5.2.1 Grid creation

The grid data (1km$^2$) is created using the investigation tool of QGIS. The number of grids is 13,392 in this implementation.

### 5.2.2 Line and Point (Vector data)

Line and point data (e.g. transportation data) are processed to the calculable form by the following steps with shape files.

Step 1: Count the numbers of lines and points and convert them to the value of each grid

### 5.2.3 Polygon (Vector data)

Polygon data (e.g. disaster occurrence) is processed to the calculable form by the following steps with shape files.

Step 1: Calculate the centroids (points) to each polygon.

Step 2: Count the numbers of centroids (points) and convert them to the value of each grid.

### 5.2.4 Image data (Raster data)

Satellite image data (e.g. forest distribution) is processed to the calculable form by the following steps.

Step 1: Extract Band 2, 3, 4, and 5 of 10 cloud cover in the area to be analyzed from LANDSAT8 in LandBrowser [9]

Step 2: Calculate the Normalized Difference Vegetation Index (NDVI) using Band 5 (near infrared NIR) and Band 4 (visible light red R) using the following formula using Raster Calculator

$$NDVI = (NIR-R)/(NIR+R)$$

Step 3: Construct virtual raster in QGIS using Band 2, 3, 4, and 5

Step 4: change the virtual raster to False Color using color-lamps

Step 5: Convert the raster data to polygon data (Polygonization)

Step 6: Calculate the centroids (points) to each polygon

Step 7: Count the numbers of centroids (points) and convert them to the value of each grid

### 5.2.5 Total Risk-Resilience Calculation

Step 1: Time-series grid-layers of each variable are integrated by "spatial join of attributes" using data id. In this implementation, we select "equals" from geometric relations such as "intersects", "overlaps", "contains", "within", "crosses" and "touches" [35].

Step 2: For the Time-series Calculation, the difference between two input layers is calculated, and for Multilayer Calculation, the accumulation among multiple layers is performed.

## 6 Experiments

To examine the feasibility of the proposed method, we conducted several experiments using the time-series data of forest-related disasters in Ibaraki prefecture in the Kanto region of Japan (2015-2020) as an example. For the purpose of evaluating the role of forests in urban disaster resilience, we define the relationship between forests, urban development, and natural disasters as "forest-urban-disaster resilience," and describe a method to analyze and visualize the time-

series of vegetation and forest distribution in urban areas using unevenly distributed time series geographic data, socio-economic indicator data, and natural disaster data.

First, we set a vulnerability for disaster as an explanatory variable $y$, and 1) disaster risk/hazard, 2) population density, 3) transportation (high-way) density, 4) forest distribution as objective variables $x_1$, $x_2$, $x_3$ and $x_4$. Second, we conduct experiments to examine the Multilayer Calculation function using the data of 2015 and the Time-series Calculation function using the data 2015 and 2020. Third, we examine the total risk values to analyze the relation among a vulnerability for disaster and 1) disaster risk/hazard, 2) population density, 3) urban infrastructure development and 4) forest distribution. Finally, we discuss the feasibility of our method to accurately assess the importance of forests and their effects and impacts.

Experiment 1: Examination on the Multilayer Calculation function
Experiment 2: Examination on the Time-series Calculation function
Experiment 3: Examination on the Total Risk-Resilience Calculation function

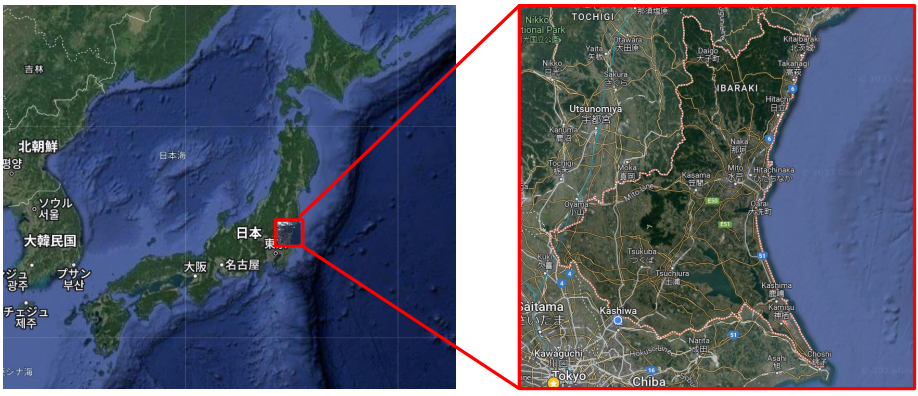


**Figure 6: Target area for analysis (Ibaraki prefecture, Japan)**
Source: own.

Data for experiments are:

- Disaster Data 1: 2015 & 2020 Landslide Disaster Precaution Area Data (Polygon, Shape file) obtained from National Land Data [13].

- Disaster data 2: 2015 & 2020 Flood Inundation Assumed Inundation Area Data (Polygon Shape file) obtained from National Land Information [14], Ministry of Land, Infrastructure, Transport and Tourism.
- Demographic data: Population distribution data of the Tokyo metropolitan area in 2015 & 2020 obtained from the Ministry of Land, Infrastructure, Transport and Tourism's National Land Survey Data [11] (Grid, Population Projection by 1km mesh of the National Land Survey Data (H30 National Bureau Estimates)).
- Urban infrastructure data: 2020 expressway time series data (Line and points, Shape file) obtained from National Land Information [12], Ministry of Land, Infrastructure, Transport and Tourism.
- Forest distribution data: satellite Landsat8 multispectral images (GeoTiff data) of Kanto region in 2015 and 2020 obtained from USGS [36] and Copernicus Open Access Hub [41].

### 6.1 Experiment 1: Examination on the Multilayer Calculation of the Risk-Resilience of Environmental Phenomena

**Figure 7** shows the original geographical information data of Ibaraki area in 2015. (a) Disaster Risk (Polygon, Vector data), (b) Population (Grid, Vector data), (c) Highway (Line and Point, Vector data), Vegetation (NDVI, Raster data) and (d) Forest distribution (Raster data) are shown.

**Figure 8** shows the same data shown in Figure 7 converted to a grid form by a data processing method described in Section 5.2. By this process, distributed and heterogeneous data are normalized and become calculable. We can grasp that the disaster risk are high in the northern part which is a mountainous area close to Tochigi prefecture, the population density is high in the middle part with relatively-big cities (Tsukuba-city, Mito-city, Hitachinama-city and Hitachi-city), the transportation density is high in the southern part close to Tokyo, and the forest density is high in the western part.

**Figure 9** shows the total risk calculation result by the multilayer calculation method described in Section4.2. From this result, we can observe the total risk distribution that cannot be figured from Figure 8. From Figure 8, the independent layer's values

and distribution can be observed, but total risk of each grid is difficult to estimate by human eyes. Only by this calculation, we can evaluate the total risk distribution.

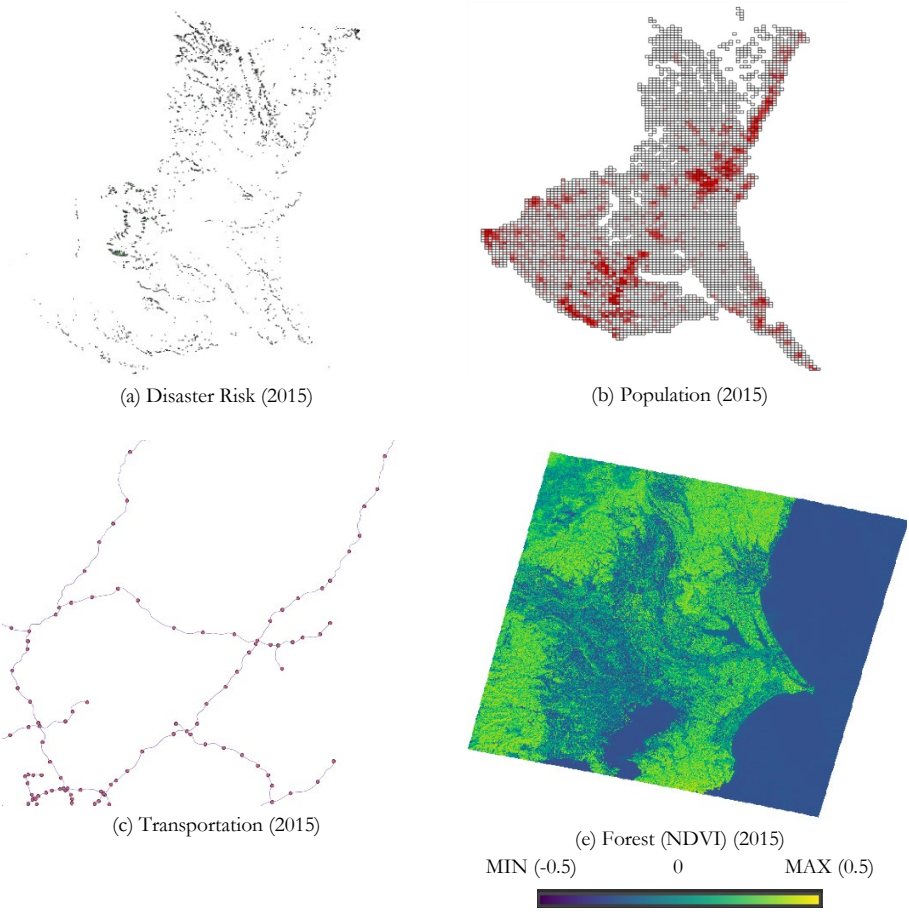


**Figure 7: Original Data of Ibaraki area in 2015: (a) Disaster Risk (Polygon, Vector data), (b) Population (Grid, Vector data), (c) Highway (Line and Point, Vector data), Vegetation (NDVI, Raster data) and (d) Forest distribution (Raster data)**
Source: own.

The results of Experiment 1 in **Figure 7 – Figure 9** show that our method enables to calculate the total risk/resilience for disasters of the target area as aggregated values with multidimensional, distributed and heterogeneous variables by a normalized grid format.

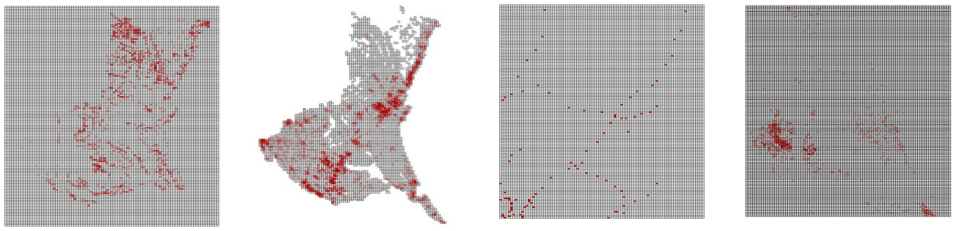

(a) Disaster Risk (2015) (b) Population (2015) (c) Transportation (2015) (d) Forest (2015)

**Figure 8: Data of 2015 in Figure 7 converted to grid data: (a) Disaster Risk, (b) Population, (c) Highway and (d) Forest distribution (NDVI)**

Source: own.

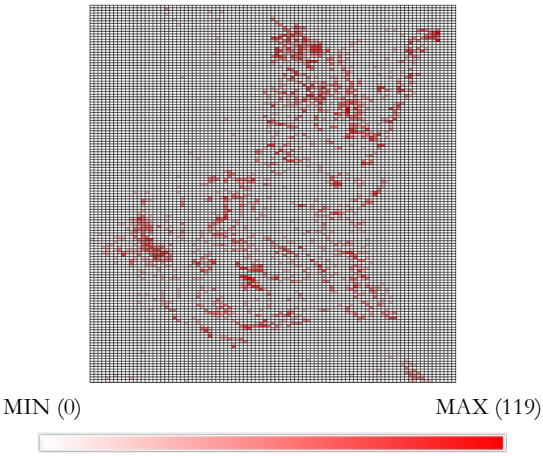


**Figure 9: Total Risk Calculation Result (without Population) in 2015**

Source: own.

## 6.2 Experiment 2: Examination on the Time-series Change Calculation of the Risk-Resilience of Environmental Phenomena

**Figure 10**, **Figure 11**, **Figure 12** and **Figure 13** show the results of time-series change calculation for geographical distribution of disaster risk, population, transportation and forest, respectively, from 2015 to 2020. From (a) 2015 and (b) 2020 of each figure, it is difficult to find the difference by human eyes. These results show that the time-series change is clearly notable with numerical values by our time-series change calculation. Also, by using a grid form, distributed and heterogeneous data are normalized and become calculable and comparative.

From **Figure 10**, we can grasp that the disaster risk increased in the northern part which is a mountainous area close to Tochigi prefecture. **Figure 11** indicates that the population density decreased in the northern coastal area around Hitachinakai-city, where a big Tsunami hit in 2011, and increased in the southern part around Tsukuba-city. **Figure 12** shows that highway junctions increased a few in the southern part close to Tokyo. **Figure 13** show that forest and vegetation are decreased seriously in the western part close to Saitama prefecture and newly developing cities (Shimotsuma-city and Yachiyo-city). These changes might be happened from land use change from agricultural area to housing area because the western part of Ibaraki is a large field of rice and vegetables.

The results of Experiment 2, shown in **Figures 10 through 13**, indicate that this method can be used to calculate the time-series change of each variable in a normalized grid format among a multidimensional, distributed and heterogeneous set of variables of disaster risk/resilience in the target area.

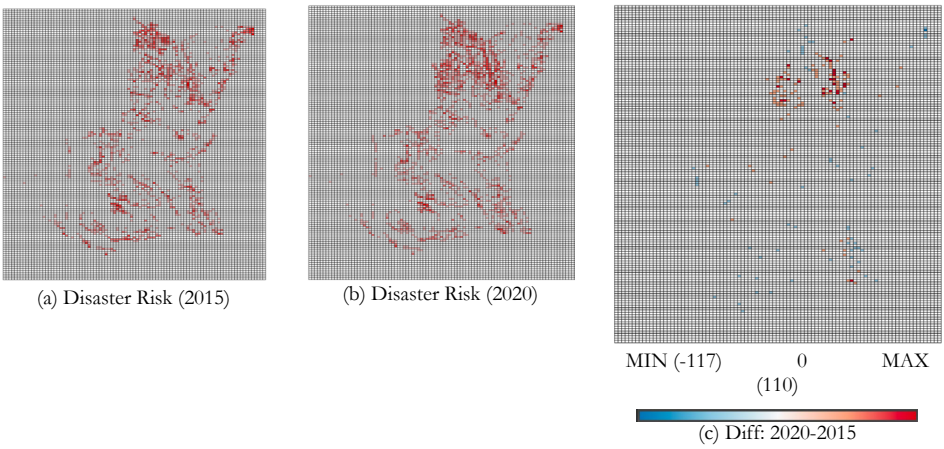


**Figure 10: Time-series Change Calculation of Disaster Risk (2020-2015): (a) disaster risk in 2015, disaster risk in 2020, (c) increase or decrease in disaster risk value (grid expression, increase: red, decrease: blue)**

Source: own.

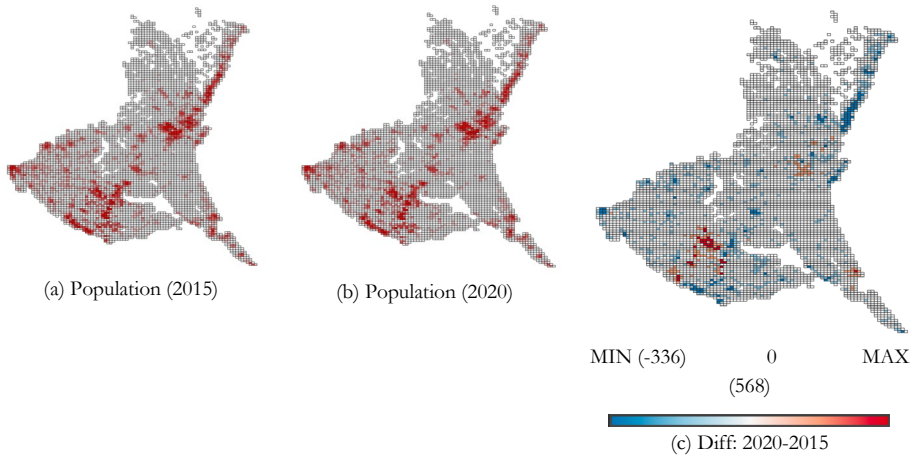


**Figure 11: Time-series Change Calculation of Population (2020-2015): (a) population in 2015, population in 2020, (c) increase or decrease in population value (grid expression, increase: red, decrease: blue)**

Source: own.

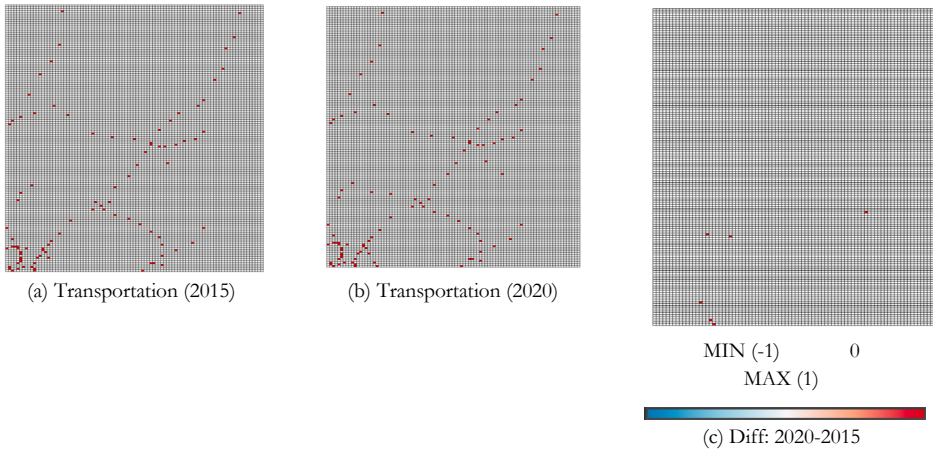


**Figure 12: Time-series Change Calculation of Transportation (2020-2015): (a) highway junctions in 2015, highway junctions in 2020, (c) increase or decrease in the number of highway junctions (grid expression, increase: red, decrease: blue)**

Source: own.

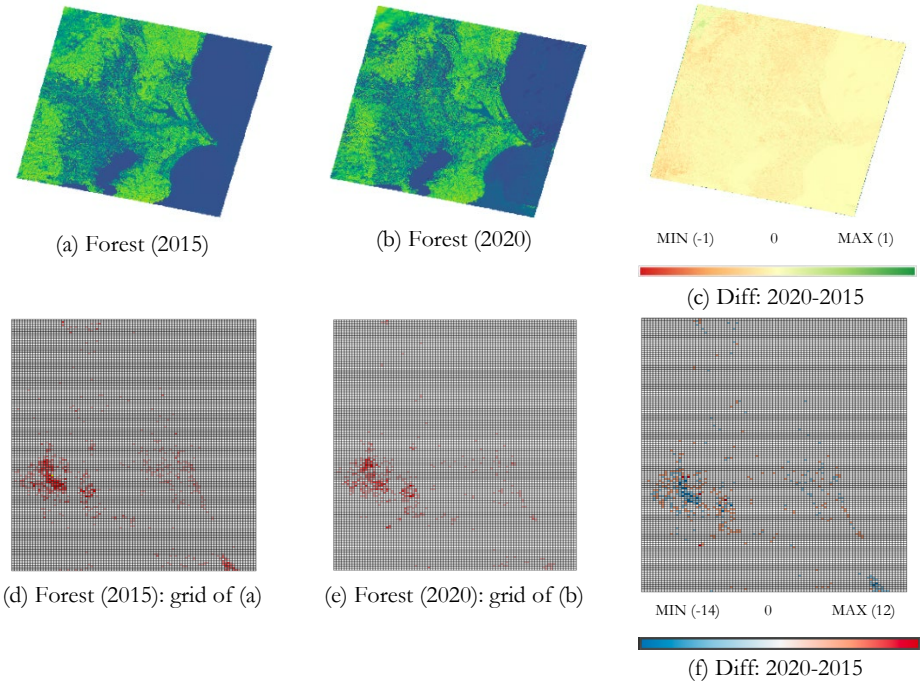


**Figure 13: Time-series Change Calculation of Forest Distribution (2020-2015) : (a) forest distribution (NDVI) in 2015, (b) forest distribution (NDVI) in 2020, (c) increase or decrease of forest areas (increase: green, decrease: red), (d) forest distribution (grid expression) in 2015, (b) forest distribution (grid expression) in 2020, (c) increase or decrease of forest areas (grid expression, increase: red, decrease: blue)**
Source: own.

Experiment 3: Examination on the Time-series Multilayered Calculation of the Risk-Resilience of Environmental Phenomena

Experiment 3 is a combination of the results of Experiment 1 and 2. **Figure 14** shows the result of the total risk-resilience calculation by the Time-series Multilayered Calculation method described in Section 4.2 and Section 4.3. In this calculation, we did not include population density data because we judge that it is difficult to define if a population growth contributes to disaster resilience or not. **Figure 15** shows an overlay result of Ibaraki-pref. base map [43] on the result shown in Figure 4 for a reference. **Figure 16** shows the visualization and sharing of the result of Figure 14 on 5D World Map System and **Figure 17** shows the same result on Google Earth. From these results, we can observe that the vulnerability to

disasters increased in the red part (the northern part of Ibaraki) and decreased in the blue part (the western part of Ibaraki). Conversely, the result can be interpreted that the resilience to disasters increased in the blue part (the western part of Ibaraki) and decreased in the red part (the northern part of Ibaraki).

The results of Experiment 3 in **Figures 14** and **Figure 15** show that our method enables to transform multidimensional, distributed and heterogeneous variables into a form that allows comparative and arithmetic operations through a normalization process, by reflecting the amount of change in each variable in the past to calculate a total aggregate value of risk/resilience to disaster in a specific target area. **Figure 16** and **Figure 17** show that the results by our method can be shared on the common Web application such as Google Earth or 5D World Map System to be utilized for designing disaster-countermeasure and policies in local governments.

To increase the degree of accuracy and precision, it seems to be important to add more variables such as land use for houses, agriculture, manufacture, commercial malls, power plants and dams as infrastructure parameters and socioeconomic parameters. Also, natural parameters such as the amount of rainfall, humidity and snowfall, the frequency of serious earthquakes and forest fires should be added.

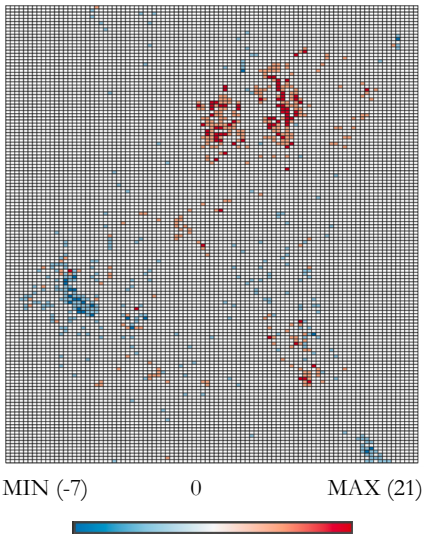


(f) Diff: 2020-2015

**Figure 14: Total Risk-Resilience Calculation results by the Time-series Multilayered Calculation (Ibaraki prefecture in Japan, 2015-2020)**

Source: own.

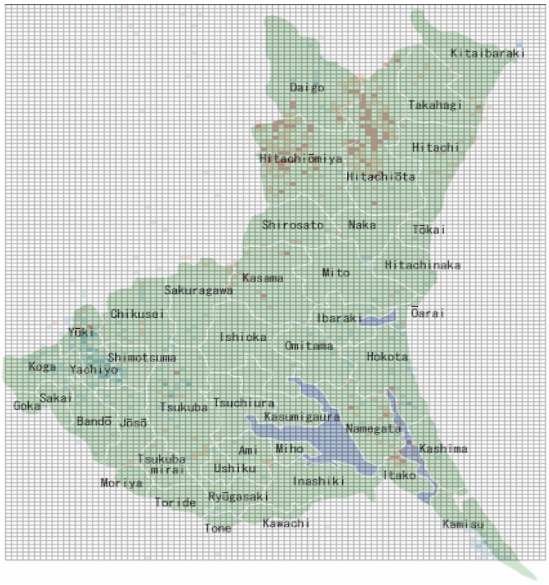


**Figure 15**: **Overlay result of Ibaraki-pref. base map [43] on the result shown in Figure 4.**

Source: own & [43].


**Figure 16: Mapping of the total risk-resilience calculation result as a KML/KMZ file for visualization and sharing on 5D World Map System**

Source: own.

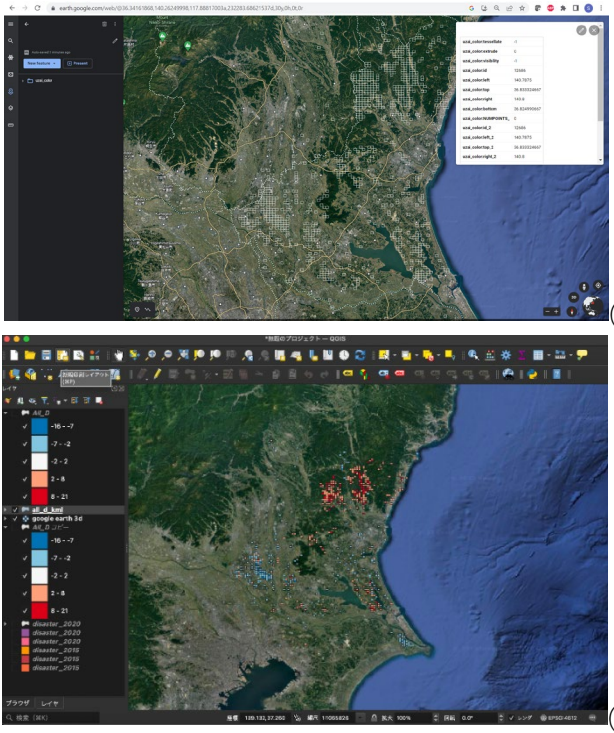


**Figure 17: Mapping of the total risk-resilience calculation result for visualization and sharing on Google Earth [44]: (a) Mapping of a KML/KMZ file on Google Earth, (b) Mapping of shape file on QGIS with a Google Earth BaseMap**

Source: own.

## 7 Conclusion and Future Direction

In this paper, "Time-series Multilayer Risk-Resilience Calculation" method for global environmental change and disaster analysis has been presented. Through the implementation and experiments, it is examined that our method enables to transform multidimensional, distributed and heterogeneous variables into a form that allows comparative and arithmetic operations through a normalization process, by reflecting the amount of change in each variable in the past to calculate a total aggregate value of risk/resilience to disaster in a specific target area.

As a future development, we will implement an automatic disaster estimation and prediction system using open data to realize a disaster resilience improvement system integrated with 5D World Map System.

Future issues include an addition of explanatory variables such as land use for houses, agriculture, manufacture, commercial malls, power plants and dams as infrastructure parameters and socioeconomic parameters, and natural parameters such as the amount of rainfall, humidity and snowfall, the frequency of serious earthquakes and forest fires etc. to increase the degree of accuracy and precision of our method.

The goal of our research is to support the realization of SDG9, SDG13, SDG11 and SDG15 in countries and regions around the world, especially in the Least Developing Countries (LDCs) that lack advanced observation equipment, technology, and financial resources. Specifically, the project will be developed with evaluation of relationships among multiple variables, and disaster prediction. We will develop our method to build a system that can predict potential disaster locations and vulnerable locations by integrating elements divided into the specific research fields.

**Acknowledgement**

We appreciate the members of ICT & Disaster Risk Reduction Division (IDD), UN ESCAP and Asia AI Institute (AAII), Musashino University and Thammasat University for the significant discussions on this study.

**References**


[1] Kiyoki, Y. and Chen, X., "Contextual and Differential Computing for the Multi-Dimensional World Map with Context-Specific Spatial-Temporal and Semantic Axes." Information Modelling and Knowledge Bases XXV 260 (2014): 82.

[2] Kiyoki, Y., Chen, X., Sasaki, S., Koopipat, C., "A Globally-Integrated Environmental Analysis and Visualization System with Multi-Spectral & Semantic Computing in "Multi-Dimensional World Map"", Information Modelling and Knowledge Bases XXVIII, pp.106-122,2017.

[3] Sasaki, S., Takahashi, Y, Kiyoki, Y., "The 4D World Map System with Semantic and Spatiotemporal Analyzers," Information Modelling and Knowledge Bases, Vol.XXI, IOS Press, pp. 1 - 18, 2010.

[4] Sasaki, S. and Kiyoki, Y., "Real-time Sensing, Processing and Actuation Functions of 5D World Map System: A Collaborative Knowledge Sharing System for Environmental Analysis" Information Modelling and Knowledge Bases, Vol. XXVIII, IOS Press, pp. 220-239, May 2016.

[5] Sasaki, S. and Kiyoki, Y., "Analytical Visualization Functions of 5D World Map System for Multi-Dimensional Sensing Data", Information Modelling and Knowledge Bases XXIX, IOS Press, pp.71 – 89, May 2017.

[6] Kiyoki, Y., Chen, X., C., Rachmawan, I. E. W., Chawakitchareon, P., "A SPA-based Semantic Computing System for Global & Environmental Analysis and Visualization with "5-Dimensional World-Map": "Towards Environmental Artificial Intelligence"" Information Modelling and Knowledge Bases XXXI, Vol. 321, pp. 285 – 305, DOI 10.3233/FAIA200021, IOS Press, 2020.

[7] Sasaki, S., Kiyoki, Y, Sarkar-Swaisgood, M., Wijitdechakul, J., Rachmawan, I. E. W.., Srivastava, S., Shaw, R. and Veesommai, C., "5D World Map System for Disaster-Resilience Monitoring from Global to Local: Environmental AI System for Piloting SDG 9 and 11", Information Modelling and Knowledge Bases XXXI, Vol. 321, pp. 306 - 323, DOI 10.3233/FAIA200022, IOS Press, 2020.

[8] Uraki, A., Sasaki, S. and Kiyoki, Y., "A Multi-dimensional Visualization Method for Disaster Analysis on 5D World Map System", 2018 Int'l Electronics Symposium (IES-KCIC), 139-145, 2018.

[9] Kiyoki, Y, Chen, X., "A Semantic Associative Computation Method for Automatic Decorative-Multimedia Creation with "Kansei" Information" (Invited Paper), The Sixth Asia-Pacific Conferences on Conceptual Modelling (APCCM 2009), 9 pages, January 20-23, 2009.

[10] Chen, X., Kiyoki, Y., "A Semantic Orthogonal Mapping Method through Deep-learning for Semantic Computing", Information Modelling and Knowledge Bases XXX, Vol.312, pp.39 – 60, DOI 10.3233/978-1-61499-933-1-39, IOS Press, 2019.

[11] Kiyoki, Y., Chawakitchareon, P., Rungsupa, S., Chen, X., Samlansin,K., "A Global & Environmental Coral Analysis System with SPA-Based Semantic Computing for Integrating and Visualizing Ocean-Phenomena with "5-Dimensional World-Map", INFORMATION MODELLING AND KNOWLEDGE BASES XXXII, Frontiers in Artificial Intelligence and Applications 333, IOS Press, pp. 76 – 91, Dec 2020.

[12] Rachmawan, I. E. W. and Kiyoki, Y., "A New Approach of Semantic Computing with Interval Matrix Decomposition for Interpreting Deforestation Phenomenon", Information Modelling and Knowledge Bases XXX, Vol.312, pp.353 – 368, DOI 10.3233/978-1-61499-933-1-353, IOS Press, 2019.

[13] Wijitdechakul, J. and Yasushi Kiyoki, Chawan Koopipat, "An environmental-semantic computing system of multispectral imagery for coral health monitoring and analysis", Information Modelling and Knowledge Bases XXX, Vol.312, pp.293 – 311, DOI 10.3233/978-1-61499-933-1-293, IOS Press, 2019.

[14] Rachmawan, I. E. W. and Kiyoki, Y., "Semantic Multi-Valued Logic for Deforestation Phenomena Interpretation", Information Modelling and Knowledge Bases XXXI, Vol. 321, pp. 401 - 418, DOI 10.3233/FAIA200027, IOS Press, 2020.

[15] Veesommai, C., Kiyoki, Y. and Sasaki, S., "A Multi-Dimensional River-Water Quality Analysis System for Interpreting Environmental Situations", Information Modelling and Knowledge Bases XXVIII, pp.43-62, 2017.
[16] Wijitdechakul, J., Kiyoki, Y., Sasaki, S., Koopipat, C., "A Multispectral Imaging and Semantic Computing System for Agricultural Monitoring and Analysis", Information Modelling and Knowledge Bases XXVIII, pp.314-333,2017.
[17] Rachmawan, I. E. W. and Kiyoki, Y.," Semantic Spatial Weighted Regression for Realizing Spatial Correlation of Deforestation Effect on Soil Degradation", International Electronics Symposium on Knowledge Creation and Intelligent Computing (IES-KCIC), September 26,2017, Surabaya Indonesia.
[18] Wijitdechakul, J., Kiyoki, Y., Sasaki, S. and Koopipat, C., "UAV-based Multispectral Aerial Image Retrieval using Spectral Feature and Semantic Computing", International Electronics Symposium on Knowledge Creation and Intelligent Computing (IES-KCIC), September 26,2017, Surabaya Indonesia.
[19] UNDRR, "Implementing the Sendai Framework", SF and the SDGs, Accessed: Jan. 30, 2023. [Online]. Available: https://www.undrr.org/implementing-sendai-framework/sf-and-sdgs
[20] UNDRR, Sendai Framework, Accessed: Jan.30, 2023. [Online]. Available: https://www.undrr.org/publication/sendai-framework-disaster-risk-reduction-2015-2030
[21] NIED, J-SHIS Map, Accessed: Jan. 30, 2022. [Online]. Available: https://www.j-shis.bosai.go.jp/map/
[22] UNEP, Global Risk Data Platform, Accessed: Jan. 30, 2022. [Online]. Available: https://preview.grid.unep.ch/
[23] UNDRR, Prevention Web, Accessed: Jan. 30, 2022. [Online]. Available: https://www.preventionweb.net/
[24] UNDRR, Global Assessment Report on Disaster Risk Reduction, Accessed: Jan. 30, 2022. [Online]. Available: https://gar.undrr.org/
[25] NICT, ARIA project , Accessed: Jan. 30, 2022. [Online]. Available: https://testbed.nict.go.jp/interview/007_1.html
[26] M. Kawamura, K.Tsujino, Y. Ohtsuji, "Investigation of Sediment Disaster Mitigation GIS by Using Results of Large Area Disaster Characteristic Analysis," Journal of Disaster Science and Management, Vol.25(1), 2006, pp.35-50.
[27] H. Kasa, M. Kurodai, S. Obayashi, H. Kojima, "On the Applicability of Remote Sensing Data for Landslide Prediction Model," Journal of the Remote Sensing Society of Japan, Vol.12(1), 1992, pp.5-15.
[28] R. Furuda, GIS and satellite image analysis with QGIS (Part 3: Basic functions, Part 2), Information Geology, vol. 29, no. 4, pp. 141-149, 2018. (Japanese)
[29] M. Miyamoto, Causes of tropical deforestation: Reconsidering slash-and-burn, population growth, poverty, and road construction, Jirinshi (2010) 92: 226-234. (Japanese)
[30] Katsuhide Yokoyama, Hiroto Tauchi, Hideo Amaguchi, Akira Kawamura, Study on the relationship between urbanization on steep slopes and landslide disasters in Japan (Japanese)
[31] ESCAP SDGHELPDESK: https://sdghelpdesk.unescap.org/
[32] Closing-the-Loop - ESCAP: https://www.unescap.org/projects/ctl
[33] Kiyoki, Y., Sasaki, S. and Barakbah, A.R., "AI-Sensing Functions with SPA-based 5D World Map System for Ocean Plastic Garbage Detection and Reduction ", Information Modelling and Knowledge Bases XXXIV, Jan. 2023. DOI:10.3233/FAIA220489
[34] Nakamura, Y. and Sasaki, S., "Disaster-Affected Area Estimation Method with Open Multispectral-Image Data Analysis for Multidimensional World Map System ", ICBIR 2022 - 2022 7th International Conference on Business and Industrial Research, Proceedings, 616-621, Jun, 2022.
[35] Max J Egenhofer, David M. Mark, Modeling conceptual neighborhoods of topological relations, Geographical Information Systems 9(5):555-565, DBLP, September 1995.
[36] USGS: https://www.usgs.gov/

[37] Ministry of Land, Infrastructure, Transport and Tourism, National Land Numerical Data, Future Population Estimates by 1km Mesh (H30 National Bureau Estimates) (shape format version), in Japan (Japanese) https://nlftp.mlit.go.jp/ksj/gml/datalist/KsjTmplt-mesh1000h30.html
[38] Ministry of Land, Infrastructure, Transport and Tourism, National Land Numerical Data, Expressway Time Series Data, in Japan(Japanese) https://nlftp.mlit.go.jp/ksj/gml/datalist/KsjTmplt-N06-v1_2.html
[39] Ministry of Land, Infrastructure, Transport and Tourism, National Land Numerical Data, Flood Inundation Assumption Area Data, in Japan (Japanese) https://nlftp.mlit.go.jp/ksj/gml/datalist/KsjTmplt-A31-v2_1.html
[40] Ministry of Land, Infrastructure, Transport and Tourism, National Land Numerical Data, Landslide Disaster Precaution Area Data, in Japan (Japanese) https://nlftp.mlit.go.jp/ksj/gml/datalist/KsjTmplt-A33-v1_4.html
[41] Copernicus Open Access Hub, Open Hub: https://scihub.copernicus.eu/dhus/#/home
[42] QGIS: https://qgis.org/ja/site/
[43] City, town, and village offices in Ibaraki prefecture: https://www.pref.ibaraki.jp/bugai/kokusai/tabunka/en/administration/level.html
[44] Google Earth: https://earth.google.com/